Tracking Closed Streamlines in Time-Dependent Planar Flows

Thomas Wischgoll   Gerik Scheuermann
Hans Hagen

University of Kaiserslautern
Department of Computer Science, Computer Graphics & CAGD
P.O. Box 3049, D-67653 Kaiserslautern, Germany
E-mail: [wischgol|scheuer|hagen]@informatik.uni-kl.de

Abstract

Closed streamlines are a missing part in most visualizations of vector field topology. In this paper, we propose a method which detects closed streamlines in a time-dependent two-dimensional flow and investigates the behavior of these closed streamlines over time. We search in all timesteps for closed streamlines and connect them to each other in temporal order to get a tube shaped visualization. As a starting point for our investigation we look for changes of the type of critical points that lead to the creation or vanishing of closed streamlines (Hopf bifurcation). We follow the resulting limit cycle over time. In addition, changes of the topological skeleton, built by critical points and separatrices, are considered which may start or terminate the life of a closed streamline.

1 Introduction

An intuitive and often used method for vector field visualization is the calculation of streamlines. They can be used to create the so called topological skeleton. This is a graph which connects the critical points, where the vector field is zero, with streamlines called separatrices. If this technique is used in turbulent fields, one encounters often the problem of closed streamlines. The difficulty with standard integration methods is that streamlines approaching a closed curve cycle around that curve without ever approaching a critical point or the boundary. Usually, one uses a stopping criterion like elapsed time or number of integration steps to prevent infinite loops. But we are interested in the exact location of the closed streamlines. Therefore such a vague criterion does not fit our needs. For this reason we developed an algorithm [16] that uses the underlying grid to check if the same cell is entered again while integrating the streamline: this results in a cycle of cells. In that case, the algorithm determines if the streamline can leave this cell cycle or not. If it does not leave it is proven that there exists a closed streamline inside the cell cycle if there is no critical point inside the involved cells. This proof is based on the famous Poincaré-Bendixson-theorem in dynamical systems theory.

In time-dependent planar flows it is possible to track the paths of the critical points and draw the separatrices as surfaces that vary when time propagates [13]. When following one particular critical point, for instance a sink, this critical point may switch its type and becomes a source. This kind of structural change is called Hopf bifurcation. This is only possible if there emerges or vanishes a closed streamline in the surrounding of the critical point. Then, the separatrix does not reach the critical point anymore but ends at the closed streamline instead as shown in figure 1.

For a better understanding of these essential topological properties of time dependant vector fields we investigate the evolution of closed streamlines over time. We will describe two different types of structural changes (bifurcations) which start or terminate the life cycle of a closed streamline: one is the Hopf bifurcation mentioned above. The other structural change is the blue sky in 2D bifurcation where a saddle gets connected to itself by a streamline. This bifurcation is called global because it does not involve a change of a critical point but a change of the connectivity of separatrices in the topological skeleton.

The evolution of closed streamlines in planar flows is visualized by a third dimension representing time. We can show the evolution using a tube that interpolates a closed streamline at dif-

ferent timesteps. This technique was inspired by *The Visual Mathematics Library* by Abraham and Shaw [1] which facilitates a great way to understand dynamics by the use of discerning sketches.

In the next section we summarize previous work. Afterward, we simmarize the necessary theoretical background and introduce critical points and the different types of bifurcations concerning the creation or termination of closed streamlines in section 3. Section 4 describes the algorithm that detects closed streamlines and finds their exact location. Then we describe how to construct a tube shaped surface representing the evolution of the closed streamline over time in section 5 while section 6 shows the results of our method using a real world example. Section 7 concludes and gives some ideas for future work.

2 Related Work

From the mathematical point of view, *The Visual Mathematics Library* by Abraham and Shaw [1] has presented dynamical systems in a way that is easy to understand by drawing discerning sketches. In particular, for depicting the evolution of closed streamlines in a two-dimensional time-dependent vector field, the third space dimension is used. Furthermore, the practical significance of unsteady flow fields has led to several techniques for the visualization of time-dependent vector fields without considering closed streamlines. A method for computing streaklines in 3D unsteady flow fields has been proposed [11]. The basic principle is to integrate streaklines thanks to an interpolation over the 3D space and time. The technique works also with moving grids. Using this scheme, a method for displaying unsteady flow volumes has been presented by Becker et al. [2]. Based upon an adaptive subdivision strategy, the authors arrive at integrating streaklines starting on a generating polygon. *Spot noise* also has been extended by de Leeuw et al. [4] to handle time-dependent planar vector fields. For the purpose of feature visualization, Silver [12] tracks and correlates the extracted structures of isosurfaces by detecting the following fundamental events: continuation, bifurcation, amalgation, creation and dissipation. Tricoche et al. [13] present a method for displaying time-dependent topology by tracking critical points over time and computing separatrix surfaces representing the evolution of

topology. In some constellations, the critical points can be a hint for closed streamlines.

The first two authors presented an algorithm that computes streamlines while detecting if it runs into a closed streamline in two dimensional flows [16]. This can also be used in the time slices of a time-dependent dataset. Haimes discusses a similar problem [7] where residence time is used to find recirculation regions. When reaching a closed streamline the residence time is infinite. The problem of closed streamlines is also related to the study of dynamical systems [6], [9] which have also been an application area for visualization. Hepting et al. [8] study invariant tori in four-dimensional dynamical systems by using suitable projections into three dimensions to enable detailed visual analysis of the tori. Wegenkittel et al. [15] present visualization techniques for known features of dynamical systems. Bürkle et al. [3] use a numerical algorithm developed by some of the coauthors [5] to visualize the behavior of more complicated dynamical systems. In the numerical literature, we can find several algorithms for the calculation of closed curves in dynamical systems [10], [14], but these algorithms are tailored to deal with smooth dynamical systems where a closed form solution is given and an artificial grid is introduced including expensive refinements. In contrast, visualization faces far more often piecewise linear or bilinear vector fields. Here, the knowledge of the grid and the linear structure of the field in the cells allow a direct approach for the search of closed streamlines without refining the underlying grid.

3 Theory

The topological analysis of vector fields considers the asymptotic behavior of streamlines. The origin set or α-limit set of a streamline c is defined by

$$\{p \in \mathbb{R}^2 \, | \, \exists (t_n)_{n=0}^{\infty} \subset \mathbb{R}, t_n \to -\infty,$$
$$\lim_{n \to \infty} c(t_n) \to p\}.$$

The end set or ω-limit set of a streamline α is defined by

$$\{p \in \mathbb{R}^2 \, | \, \exists (t_n)_{n=0}^{\infty} \subset \mathbb{R}, t_n \to \infty,$$
$$\lim_{n \to \infty} c(t_n) \to p\}.$$

If the α- or ω-limit set of a streamline consists of only one point, this point is a critical point or a point at the boundary ∂D of our domain D. (It is

assumed that the streamline stays at the boundary point forever in this notation.) The critical points can be clearly identified because they are simply the zeros of the vector field.

The most common case of an α- or ω-limit set in a planar vector field containing more than one inner point of the domain is a closed streamline, as described in dynamical systems theory [9]. This is a streamline c_a, so that there is a $t_0 \in \mathbb{R}/\{0\}$ with

$$c_a(t + nt_0) = c_a(t) \quad \forall\, n \in \mathbb{N}.$$

Closed streamlines are introduced in the field by structural changes, called *bifurcations*. When a vector field changes over time there may be a change in the topology from one state to another. The unstable state in between is called a *bifurcation*. This change may only affect one critical point and its nearer surrounding. Then we call it a *local bifurcation*. The other case is a *global bifurcation* where the global structure of the flow is changed.

Here we consider only bifurcations that result in the creation or vanishing of a closed streamline. The main types are the *Hopf Bifurcation* which is a local bifurcation and the *Periodic Blue Sky in 2D Bifurcation* which is a global one.

3.1 Hopf Bifurcation
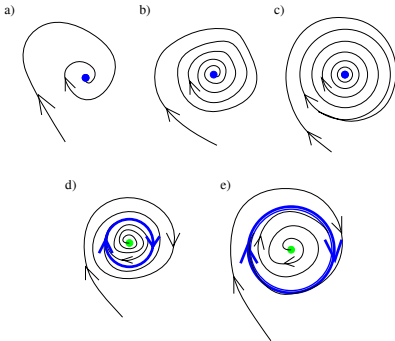
Figure 1: Hopf bifurcation

Let us assume that we are given an attracting focus as in figure 1a so that a streamline spirals around this critical point and finally converges against it. If the attracting effect weakens the number of rotations of the streamline will increases as in figure 1b. Continuing with this process the attracting

focus becomes a center point (figure 1c) which is an unstable structure: the Hopf bifurcation has occurred. Going further, the structure becomes stable again and we have now a repelling focus. Since the global structure of the flow has not changed we still have an inflow from the outside and a flow starting at the critical point. Consequently, a closed streamline appears according to the Poincaré-Bendixson-Theorem [6] as in figure 1d and 1e. Inverting the direction of time, we get a transition from a closed streamline with a repelling focus inside into an attracting focus over an instantaneous center where the closed streamlines vanishes. Similar transitions are obtained by inverting the direction of the flow, i.e. by replacing sources by sinks. (It may be noted that we can apply the Poincaré-Bendixson-theroem only if the vector field is continuous. Further we have a region without critical points.)

3.2 Periodic Blue Sky in 2D Bifurcation
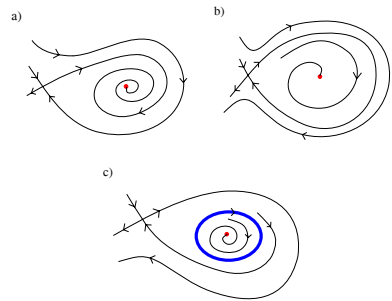
Figure 2: Periodic Blue Sky in 2D

In this type of bifurcation there are two different types of critical points involved: a saddle and an attracting focus. Figure 2a shows the situation. As the attracting effect of the focus gets weaker and weaker we see a homoclinic connection after some time where the saddle is connected to itself as shown in figure 2b. This results in a bifurcation: when this configuration breaks up again we find a limit cycle which simply appears out of the blue. The reason for the occurrence of the closed streamline is that the attracting focus is totally unaffected by the whole event. Since there is an outflow to the critical point inside and to the saddle there must be a critical point or a closed streamline in this region

according to the Poincaré-Bendixson theorem. Because of the fact that there are only the two critical points a closed streamline emerged. This configuration is shown in figure 2c. Other bifurcations of the same type can be constructed by inverting time or replacing the attracting focus with a repelling one.

3.3 Poincaré-Map

Let us assume that we have a two-dimensional continuous vector field containing one closed streamline. Then we can choose a point P on the closed streamline and draw a *cross section S* which is a line segment nowhere parallel to the vector field. This line segment is then called a *Poincaré section*. If we start a streamline at an arbitrary point x on S and follow it until we cross the Poincaré section S again, we get another point $R(x)$ on S. This results in the *Poincaré map R*. Figure 3 illustrates the situation. The left part shows the Poincaré section with the closed streamline in the middle, drawn with a thicker line. The right part displays the Poincaré map itself. Obviously the point P on the closed streamline is a fix point of the Poincaré map.
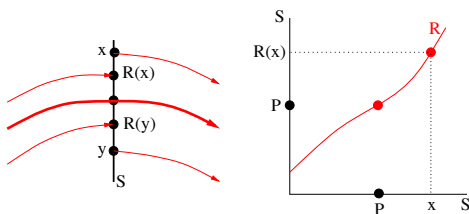
Figure 3: Poincaré section and Poincaré map.

4 Locating Closed Streamlines

As mentioned before a closed streamline $\gamma : \mathbb{R} \rightarrow \mathbb{R}^2$, $t \mapsto \gamma(t)$ is a streamline of a vector field v such that there is a $t_0 \in \mathbb{R}/\{0\}$ with $\gamma(t + nt_0) = \gamma(t) \, \forall n \in \mathbb{N}$ and γ not constant. In this section we present an algorithm that detects whether an arbitrary streamline c converges to such a closed curve. This means that c has γ as α- or ω-limit set depending on the orientation of integration. We do not assume any knowledge on the existence or location of the closed curve, so that the algorithm can detect closed streamlines. The principle of the algorithm works on any piecewise defined planar vector field

where one can determine the topology inside the pieces. The following subsections repeat the main ideas of this algorithm previously proposed by the first two authors [16].

4.1 Finding Closed Streamlines

The basic idea of the algorithm is to determine a region of the vector field that is never left by a streamline. In case of a continuous vector field the Poincaré-Bendixson-Theorem ensures that this streamline approaches a closed streamline if no critical point exists in that region. We assume that the data of the vector field is given on a grid consisting of triangles and/or quadrilaterals. The vectors inside a cell are interpolated linearly/bilinearly so that we get a continuous vector field as needed for the theorem.

A streamline approaching a closed streamline has to reenter the same cell again. In this case we check if the cells were crossed by the streamline in the same order for the last two turns. This results in a *cell cycle* which identifies the above mentioned region. To examine if this cell cycle is left by the streamline we detect possible changes by checking the edges of the cells of the cell cycle. Therefore we identify points on each edge which we call *potential exits* where an outflow out of the cell cycle may occur in the vicinity. These points are identical with the vertices of the edge and points where the vector field is tangential to the edge.
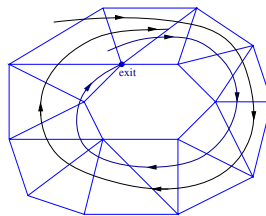
Figure 4: If a real exit can be reached, the streamline will leave the cell cycle.

Then we have to figure out if the actually investigated streamline will leave the cell cycle near such an exit. Therefore we integrate a streamline backwards from the potential exit to see if it leaves the cell cycle. If it does not leave after it crossed every cell of the cell cycle it converges to our streamline. We call this potential exit a *real exit* because

the streamline will leave the cell cycle after a finite number of turns near that exit. Figure 4 displays an example for that case.

If the backward integrated streamline leaves the cell cycle, there will also be an entry point as shown in figure 5. A streamline starting at that point cannot be crossed by our actually investigated streamline. Consequently we cannot leave the cell cycle at this exit.
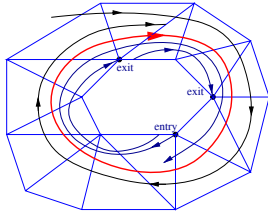
Figure 5: If no real exit can be reached, the streamline will approach a closed streamline.

If there is no real exit for the streamline, we have proven that the streamline will never leave the cell cycle. If there is no critical point inside the cell cycle the Poincaré-Bendixson-Theorem ensures that there exists a closed streamline in our cell cycle and the integral curve tends toward it.

4.2 Exact Location of the Closed Streamline

The exact position of the closed streamline can be found using the Poincaré map R. R maps the point on the closed streamline onto itself because the closed streamline will intersect the Poincaré section always at the same point. Consequently, it is sufficient to find the fix point to get a point on the closed streamline. If we find a cell cycle we can use the edge where we detected the cell cycle for the first time as a Poincaré section. To find the fix point of the Poincaré map we do a binary search: first we divide the edge into two parts at the mid point of the edge. Then we check which part gets intersected by the streamline starting at the intersection point after one turn. This part is subdivided again and we start another streamline. This continues until we are close enough at the fix point of the Poincaré map. If we start a streamline at this point we get the whole closed streamline after we crossed every cell of the cell cycle. This method terminates

because we proved in the previous step where we detected the cell cycle that we converge to a closed streamline.

5 Following Closed Streamlines

When dealing with time-dependent two-dimensional flows we can use the third dimension to represent time. We assume the vector field is given at time slices on a triangular grid. These time slices are connected using prism cells. To interpolate the vectors we consider the following map

$$f : \mathbb{R}^3 \supset D \quad \longrightarrow \quad T\mathbb{R}^2 \approx \mathbb{R}^2 \subset \mathbb{R}^3$$
$$(x, t) \quad \mapsto \quad v(x, t)$$

where D is the domain represented by the three dimensional grid. Since we need consistency with the piecewise affine linear interpolation that would be applied on a 2D triangulation, we have to ensure that the restriction of the 3D interpolant to each time plane is piecewise affine linear, too. That means that, fixing the time coordinate and taking it as a parameter, the interpolant must be affine linear. This is the reason why we choose the following interpolant inside each prism cell.

For a given prism cell lying between t_i and t_{i+1}, let $v_j(x) = A_j x b_j$, $j \in \{i, i + 1\}$ be the linear interpolation corresponding to the prism triangle faces lying in the planes $\{t = t_i\}$ and $\{t = t_{i+1}\}$ respectively. Then we define the interpolant over the whole prism cell by linear interpolation over time:

$$v(x, t) = \frac{t_{i+1} - t}{t_{i+1} - t_i} v_i(x) + \frac{t - t_i}{t_{i+1} - t_i} v_{i+1}(x)$$

where $t \in [t_i, t_{i+1}]$. This formula obviously ensures, for each fixed value of t, that $v(x, t)$ is affine linear in x.

For tracking the closed streamlines we first determine the behavior of the critical points. For a given cell, the associated interpolant contains, for each value of time t, a single critical point. This is due to the affine linear nature of its restriction to any time plane. Letting the time parameter t move from t_i to t_{i+1}, the critical point position describes a 3D curve. A detailed description of how to find the paths of the critical points can be found in the article of Tricoche et al. [13].
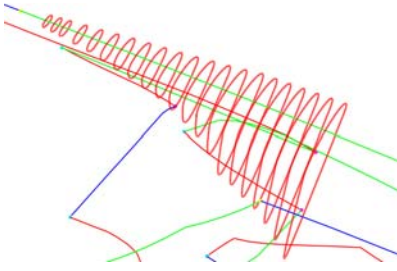
Figure 6: Closed streamlines found by the algorithm.

Figure 7: Closed streamlines visualized as a tube over time.

After that we analyze the vector field in discrete timesteps. Since there must be a critical point inside each closed streamline we use the critical point path containing a Hopf bifurcation as a starting point for our streamline algorithm from subsection 4.1 which detects the closed streamline if it exists. Therefore we follow the critical point path in discrete steps in positive and negative directions starting at the bifurcation. After we have found the cell cycle containing the closed streamline we find the exact position using the Poincaré-map from subsection 4.2. Then we have to check if the closed streamline really surrounds the critical point. This is necessary because the streamline may have ran in another closed streamline in a totally different region of the flow. Obviously, closed streamlines surrounding the critical point occur only in one of the two temporal directions. This process continues until the closed streamlines reach either another bifurcation which breaks them up or the border of the grid.

Figure 6 shows the result of this step, where we have found the closed streamlines at various timesteps. The closed streamlines are approximated by several line segments and the paths of the critical points are also shown using the same colors as in the original paper [13]. The Hopf bifurcation, where we started to detect the closed streamlines, is marked with a yellow sphere. In this example the life cycle of the closed streamline is started by a Hopf bifurcation and terminated by a Periodic Blue Sky in 2D bifurcation.

To visualize the evolution of closed streamlines, we construct tubes from the various closed streamlines similar to the pictures by Abraham and Shaw [1]. Therefore we construct surfaces consisting of triangles which connect the approximating line segments of the closed streamlines. The bifurcation
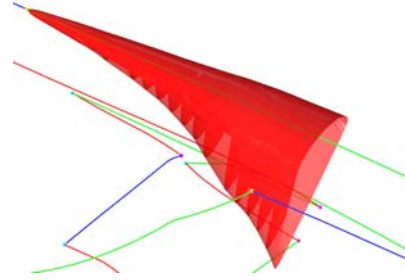
point is connected to the tube using a parabolic surface approximated with triangles. The result is shown in figure 7. We used an alpha value of 0.7 to get a better three dimensional impression and to prevent the tubes from hiding the paths of the critical points.

6   Results

To test our method, we have created a synthetic vector field containing four critical points. The position of the critical points are a function of time, describing closed curves in the plane. We have sampled this vector field on a triangular point set for several values of the time parameter. The rotation of the critical points (each with a specific frequency) entails many structural changes for the topology. This is very interesting for our purpose since all different types of bifurcations are present which create closed streamlines.

Figure 8 shows the result of our algorithm, where the closed streamlines are shown as red tubes. The upper one and the one on the right are started and terminated by Hopf bifurcations – shown as a yellow sphere – while the lower closed streamline starts at a Hopf bifurcation and is terminated by a Periodic Blue Sky in 2D bifurcation. Since there is a critical point inside the cell cycle, i.e. the saddle, the flow behaves totally different depending on where a streamline passes the saddle. Therefore the exact localization fails when we are too close to the critical point.

The next dataset is a simulation of a swirling jet with in inflow into a steady medium. The simulation uses a cylindrical domain and assumes rotational symmetry, so that we are left with a two-
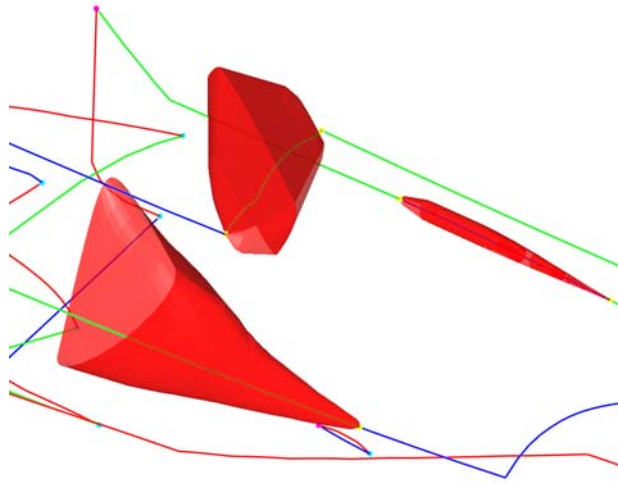
Figure 8: Closed streamlines found in a synthetic test dataset.

dimensional vector field on a plane through the center axis of the cylinder. In this application one is interested in investigating the turbulence of the vector field and in regions where the fluid stays very long. Swirling jets play a significant role in many combustion processes. It is important to find such recirculation regions indicated by closed instantaneous streamlines. To avoid visual clutter we use only a part of the dataset for our visualization. Figure 9 shows the result of our algorithm. The critical point paths are also shown where saddles are colored red, sinks are green, and sources are visualized using blue color. Obviously, in regions where only one saddle point is involved, we cannot find any closed streamlines due to the types of bifurcations explained in section 3. Most of the closed streamlines emerge at Hopf bifurcations which are marked with a yellow sphere. Therefore, closed streamlines are found where sources and sinks alternate while time propagates, so that we are able to identify the regions where the fluid stays very long.

7 Conclusions and Future Work

We presented a method to visualize the evolution of closed streamlines over time and explained the important role of bifurcations concerning the emergence respectively termination of closed streamlines. Our method detects closed streamlines auto-matically. We succeeded in creating visualizations like the ones presented in *The Visual Mathematics Library* [1].

Due to the unstable configuration of the homoclinic connection of the periodic blue sky in 2D bifurcation we actually fail to reach the bifurcation exactly. Our implementation terminates the tube representing the closed streamline slightly too early which has to be improved in the future. Another missing feature in this implementation is to find several closed streamlines around one critical point. This can be accomplished by continuing the check for closed streamlines near the last limit cycle found.

8 Acknowledgment
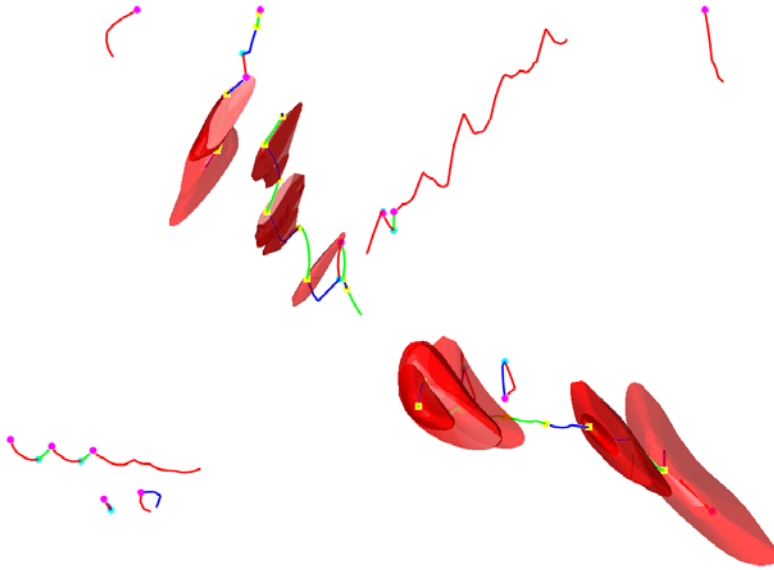
Figure 9: Closed streamlines found in a vorticity dataset.

References

[1] R. H. Abraham and C. D. Shaw. *Dynamics – The Geometry of Behaviour Part 4: Bifurcation Behaviour*. Aerial Press, Inc., Santa Cruz, 1988.

[2] B. G. Becker, D. A. Lane, and N. L. Max. Unsteady Flow Volumes. In *Proceedings IEEE Visualization 1995*. IEEE Computer Society Press, Los Alamitos CA, 1995.

[3] D. Bürkle, M. Dellnitz, O. Junge, M. Rumpf, and M. Spielberg. Visualizing complicated dynamics. In A. Varshney, C. M. Wittenbrink, and H. Hagen, editors, *IEEE Visualization '99 Late Breaking Hot Topics*, pp. 33 – 36, San Francisco, 1999.

[4] W. C. de Leeuw and R. van Liere. Spotting structure in complex time dependent flows. In H. Hagen, G. M. Nielson, and F. Post, editors, *Scientific Visualization – Dagstuhl '97*. IEEE Computer Society Press, Los Alamitos CA, 2000.

[5] M. Dellnitz and O. Junge. On the Approximation of Complicated Dynamical Behavior. *SIAM Journal on Numerical Analysis*, 36(2), pp. 491 – 515, 1999.

[6] J. Guckenheimer and P. Holmes. *Dynamical Systems and Bifurcation of Vector Fields*. Springer, New York, 1983.

[7] R. Haimes. Using residence time for the extraction of recirculation regions. *AIAA Paper 99-3291*, 1999.

[8] D. H. Hepting, G. Derks, D. Edoh, and R. R. D. Qualitative analysis of invariant tori in a dynamical system. In G. M. Nielson and D. Silver, editors, *IEEE Visualization '95*, pp. 342 – 345, Atlanta, GA, 1995.

[9] M. W. Hirsch and S. Smale. *Differential Equations, Dynamical Systems and Linear Algebra*. Academic Press, New York, 1974.

[10] M. Jean. Sur la méthode des sections pour la recherche de certaines solutions presque périodiques de syst'emes forces periodiquement. *International Journal on Non-Linear Mechanics*, 15, pp. 367 – 376, 1980.

[11] D. A. Lane. UFAT – A Particle Tracer for Time-Dependent Flow Fields. In *Proceedings IEEE Visualization 1994*. IEEE Computer Society Press, Los Alamitos CA, 1994.

[12] D. Silver. Feature visualization. In G. M. Nielson, H. Hagen, and H. Müller, editors, *Scientific Visualization Overviews – Methodologies – Techniques*, pp. 279–293. IEEE Computer Society Press, Los Alamitos CA, 1997.

[13] X. Tricoche, G. Scheuermann, and H. Hagen. Topology-Based Visualization of Time-Dependent 2D Vector Fields. *Visualization Symposium 2001*, pp. 117–126, 2001.

[14] M. van Veldhuizen. A New Algorithm for the Numerical Approximation of an Invariant Curve. *SIAM Journal on Scientific and Statistical Computing*, 8(6), pp. 951 – 962, 1987.

[15] R. Wegenkittel, H. Löffelmann, and E. Gröller. Visualizing the Behavior of Higher Dimensional Dynamical Systems. In R. Yagel and H. Hagen, editors, *IEEE Visualization '97*, pp. 119 – 125, Phoenix, AZ, 1997.

[16] T. Wischgoll and G. Scheuermann. Detection and Visualization of Closed Streamlines in Planar Flows. *IEEE Transactions on Visualization and Computer Graphics*, 7(2), 2001.